Journal of Applied Physics

RESEARCH ARTICLE | JUNE 25 2024

Electromagnetic estimation of mechanical stress in steel elements by using magnetic induction

M. A. García ; J. Vinolas ; M. S. Garcia Alonso; A. Hernando

J. Appl. Phys. 135, 245101 (2024)
https://doi.org/10.1063/5.0204626

AIP Publishing

Journal of Applied Physics ARTICLE pubs.aip.org/aip/jap

Electromagnetic estimation of mechanical stress in steel elements by using magnetic induction

Cite as: J. Appl. Phys. **135**, 245101 (2024); doi: 10.1063/5.0204626
Submitted: 22 February 2024 · Accepted: 2 June 2024 ·
Published Online: 25 June 2024

M. A. García,[1,a)] J. Vinolas,[2,3] M. S. Garcia Alonso,[3] and A. Hernando[3,4,5,6]

AFFILIATIONS

[1]Instituto de Cerámica y Vidrio (ICV), CSIC, Kelsen 5, 28049 Madrid, Spain
[2]Escuela Politécnica Superior, Universidad Francisco de Vitoria, M-515, km 1.800, 28223 Pozuelo de Alarcón, Madrid, Spain
[3]Escuela Politécnica Superior, Universidad Nebrija, C. de Sta. Cruz de Marcenado, 27, 28015 Madrid, Spain
[4]Instituto de Magnetismo Aplicado, "Salvador Velayos," UCM-CSIC-ADIF, Las Rozas, Madrid E-28230, Spain
[5]IMDEA Nanociencia, C/Faraday 9, 28049 Madrid, Spain
[6]Donostia International Physics Center, Universidad del Pais Vasco, C/Manuel de Lardizabal 5, 20018 San Sebastian, Spain

[a)]**Author to whom correspondence should be addressed:** magarcia@icv.csic.es

ABSTRACT

We present here experimental verification of a theoretical model previously developed to estimate internal mechanical stress in steel-based elements by means of non-contact electromagnetic induction measurements. Results confirm the validity of the proposed model and demonstrate that stress below 50% of the elastic limit can be detected with standard electronics.

I. INTRODUCTION

Steel is nowadays the most important structural material due to its outstanding mechanical properties,[1] and it represents the most used structural material in the world. The annual world production of steel is over 2000×10^6 tons[2] and its production accounts for 6%–7% global emissions of greenhouse gases,[3] and, in particular, between 7% and 9% of emitted CO_2. Consequently, in order to achieve a sustainable economy model based on optimizing the use of extensive resources, development of methods to monitor and prevent failure of steel-based-facilities and, in particular, their mechanical properties is required.

Most of straight mechanical tests, as building testing, are invasive and destructive, and, in the case of facilities where the steel element is embedded (as reinforced concrete), these techniques are directly non-available.

Hence, non-invasive monitoring techniques are required since they allow preventing failures, without altering the structural properties of the elements. Although stresses in the elastic regions are small, it is required to detect them in order to avoid catastrophic fails. A set of particularly interesting non-invasive methods to analyze a mechanical state of a steel-based element are electromagnetic ones.[4,5] The fact that most of steels are ferromagnetic because of their large Fe content allows one to investigate their structure and state in a non-invasive way since most magnetic and electromagnetic (EM) measurements do not require physical contact, but they can be performed remotely due to the solenoidal character of a magnetic field. There has been an extensive work focused on the EM detection of mechanical stress on steel elements by different methods[4,5] as changes in magnetic permeability,[6,7] Barkhausen noise,[8] magnetically induced change of ultrasonic waves,[9] magnetostatic effects,[10] or alteration of eddy currents[11] among others. Hence, non-invasive, magnetic inspection magnetic methods are available. However, those methods are developed to be used at the lab or statically fixed temporarily in a facility to perform measurements.

In a previous work,[12] we analyzed the detection of inhomogeneities in steel-based elements by means of EM induction between two coils in a transmission mode (i.e., with the ferromagnetic steel element placed in between both coils) developing a model to estimate the response of the sensor depending on the particularly used arrangement. This method is contactless. This proposed model was developed to analyze configurations where there is a dominant component of stress, as it is the case of train railways, with stress due to thermal dilatation, connections to train sleepers and others. The more general case

of multiaxial stress requires the use of stress, strain, and magnetic tensors, as described in Ref. 13. Therefore, the method results suitable to inspect train railways by displacing the sensor along the track overcoming limitations of the previously developed methods.

In particular, we showed that inhomogeneities in the structure of train railways associated with welding points, train sleepers, and dilatation meetings could be fairly detected with this non-contact method.[12]

The aim of this work is to confirm that using the developed sensor to detect inhomogeneities in steel could be able to detect internal stress well below the elastic limit to prevent failure and experimentally check the validity of the proposed model to estimate such an internal stress and its degree of accuracy. This could lead to design of a new type of stress sensors, to inspect large facilities in a contactless, fast, and reliable way. For this purpose, we performed a set of experiments with different parameters and compare the results with the calculus developed using the proposed model.

II. EXPERIMENTAL

The experimental setup consisted of a ferromagnetic parallelepiped piece of SR235JR steel with dimensions $10 \times 50 \times 150\ \text{mm}^3$ placed in between two coils separated 10 mm as Fig. 1(a) illustrates.

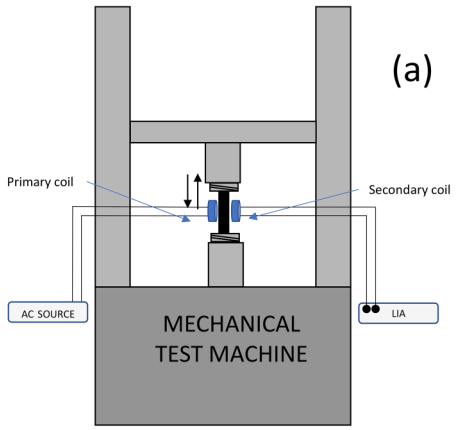

FIG. 1. (a) Sketch and (b) photo of the experimental setup.

Up to five coils with 200, 440, and 550 turns and wire diameters of 0.5 and 0.17 mm were used. Different coils were used to confirm the reliability and precision of the method as well as to look for the optimum conditions.

The source for the primary coil was adjusted to induce a 5 Vpp signal between the edges of the coil. The signal induced in the secondary coil was measured using a Lock-In amplifier SRS830 from Stanford Research Systems. A mechanical compression force was applied to the ferromagnetic steel element along the 150 mm size axis by using an EM2/200/FR mechanical properties system by Microtest. Compression forces up to 50 KN (corresponding to 100 MPa) were applied in charge–discharge cycles at controlled rates. The applied force was synchronized to the induction signal to obtain induction vs applied stress measurements. Figure 1(b) presents an overview of the developed setup.

Measurements at 1, 10, and 100 KHz of the primary coil applied signal were performed.

III. RESULTS FOR 1 KHz MEASUREMENTS

For each configuration and frequency amplitude of the signal, induced voltage in the secondary coil as well as dephasing with the signal of the primary coil were measured during mechanical charge–discharge cycles. Figures 2 and 3 present the results for six different configurations for primary and secondary coils for 1 KHz. Results for frequencies of 10 and 100 KHz (not shown) exhibited similar behavior (see the supplementary material).

The figures indicate the coincident tendency, independently of particular configuration for both modulus and phase of the induced signal. In particular, the modulus of the induced signal on the secondary coil increases with applied compression stress while dephasing between the applied and detected signal decreases for larger compression. The results indicate that both modulus and dephasing are about linear with the applied stress despite hysteresis observed for both parameters.

Table I summarizes the relevant results obtained for the different configurations.

It is noteworthy that both the relative modulus and dephasing of the signal detected at the secondary coil upon 100 MPa applied compression stress are about independent of the configuration, being of about ∼2.2% in modulus and ∼−0.48 deg in phase, which are signals easily measurable with standard electronics.

The statistical analysis of the relative modulus of the induced signal in Table I results in $(2.135 \pm 0.108) \times 10^{-2}$ (average value ± standard deviation); i.e., the dispersion is less than 10%, without a clear dependence on the number of turns of both coils. Hence, we can state that the relative values are scarcely dependent on the configuration.

Moreover, if we remove this anomalous value of the 200/550 turns (0.5 mm) that could be due to experimental errors, the statistical analysis yields $(2.21 \pm 0.11) \times 10^{-2}$, a dispersion below 5% that confirms the reliability of the method.

Similarly, the dephasing induced by the applied stress is 0.435 ± 0.08 deg, while canceling the anomalous value for 200/400 turns (0.5/0.17 mm), it is 0.466 ± 0.027 deg, again of the order of 5%.

Nevertheless, we must face that measurements shown in Figs. 2 and 3 present mechanical hysteresis, which can compromise

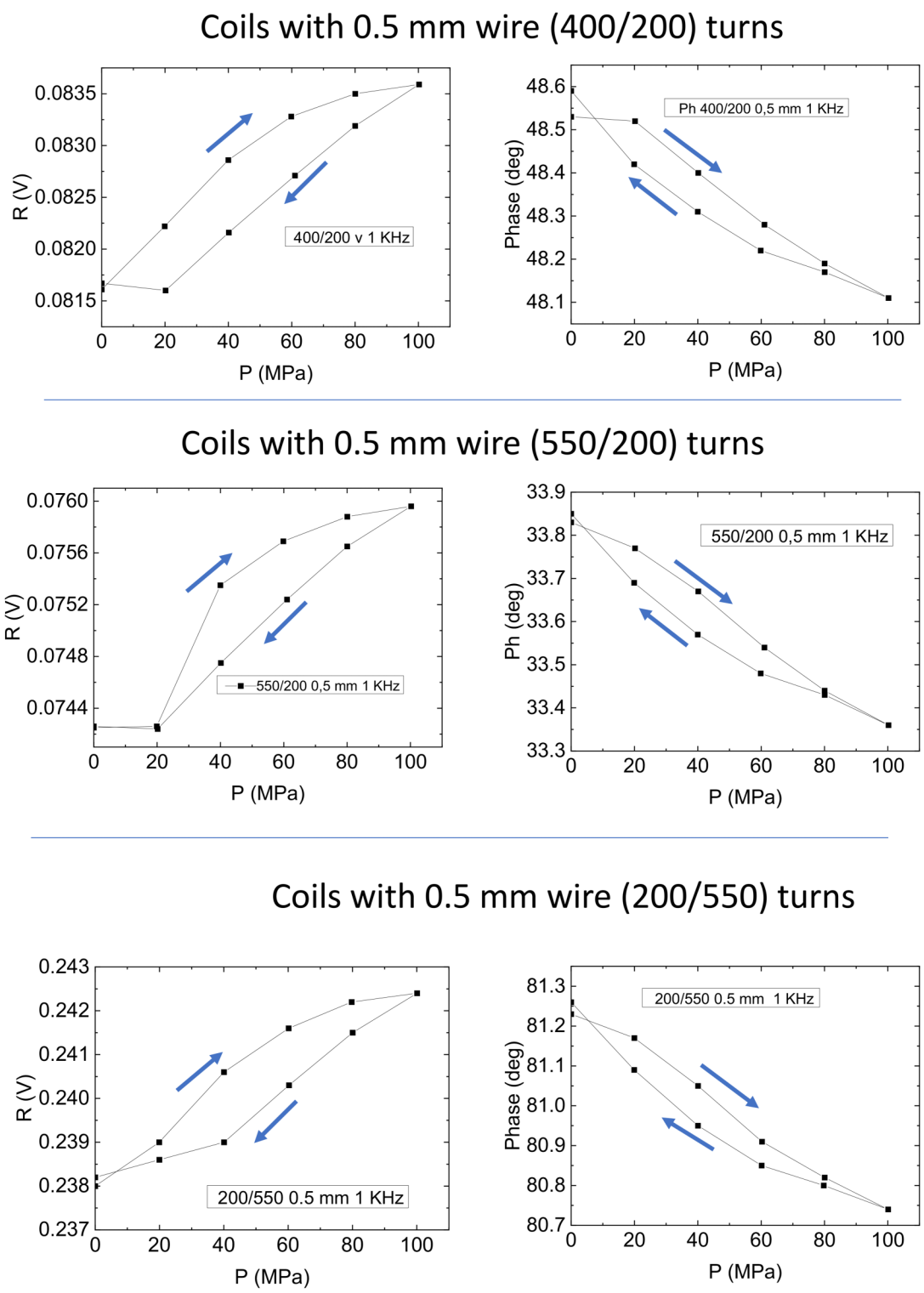

FIG. 2. Modulus and phase of the induced signal in the secondary coil as a function of applied compression stress at 1 KHz for different configurations. Arrows indicate load–unload branches.

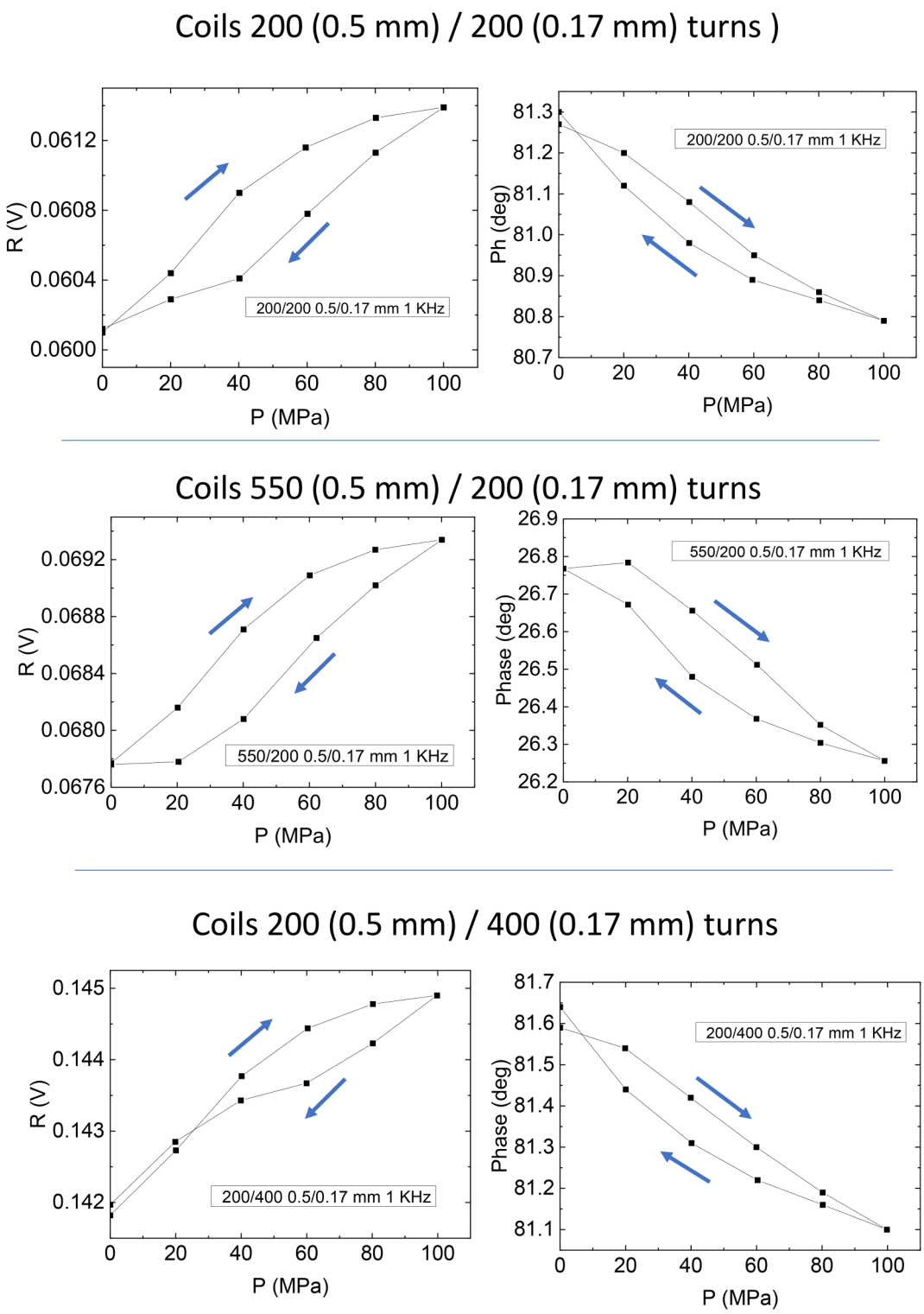

FIG. 3. Modulus and phase of the induced signal in the secondary coil as a function of applied compression stress for different configurations. Arrows indicate load–unload branches.

TABLE I. Relevant parameters obtained from the measurements presented in Figs. 2 and 3.

Config. turns (wire diam.)	R (0 MPa) (V)	R (100 MPa) (V)	ΔR/R	Φ (0 MPa) (deg)	Φ (100 MPa) (deg)	Δφ (deg)
400/200 (0.5 mm)	0.081 67	0.083 59	0.0224	48.63	48.15	−0.42
200/550 (0.5 mm)	0.074 22	0.0759	0.0176	82.19	81.70	−0.49
550/200 (0.5 mm)	0.024 28	0.2382	0.0189	81.25	80.74	−0.51
200/200 (0.5/0.17 mm)	0.060 12	0.061 39	0.0208	81.27	80.79	−0.48
550/200 (0.5/0.17 mm)	0.067 76	0.069 34	0.0233	26.79	26.29	−0.50
200/400 (0.5/0.17 mm)	0.1420	0.1450	0.0211	81.60	81.08	−0.52

the capability of the method to estimate internal stress with accuracy. Such hysteresis is similar to that detected in torsional stress experiments.[14,15] The hysteresis appearing in the magnetization as a function of cyclic applied stresses has been found to be associated with the intrinsic hysteresis of the 90° domain wall motion.[15] As it is well known, uniaxial stress induces always shear stress. This stress exert force on 90° domain walls (but not on 180° domain walls, see Ref. 16) inducing a change in the magnetic state (and, therefore, in the magnetic permeability) that remains under stress relief due to domain wall pinning mechanisms (as it happens for magnetic hysteresis).[15]

However, such hysteresis is, at maximum, 25% of the difference between signals detected at 0 and 100 MPa applied stress (which represents about ∼50% of the elastic limit of SR235JR steel, 210 MPa).[17] This hysteresis is originated by the 90° wall motion induced by the applied stress. The response of domain wall motion to magnetic fields in typically in the range of Hz, and therefore, using 1 KHz we reduce the stress associated with this effect. Moreover, if better resolution and elimination of hysteresis is required, it can be achieved, as demonstrated by Hernando *et al.*[15] for torsional experiments by applying decreasing minor loops, i.e., by demagnetizing the sample previously to carry out the measurement. The hysteresis does not prevent semi-quantitative detection of internal stress fluctuations in long steel bars, provided that the amplitude and frequency of the applied field remain constant.

Hence, those results confirm the reliability and reproducibility of the method to estimate internal stresses of steel elements well below the elastic limit. It is worthy to remark that, as previously demonstrated,[12] these measurements do not depend on the distance between each coil and the ferromagnetic element, but just on the total distance between coils. Hence, they can be done even if small vibrations or uncontrolled displacement of the analyzed element are present.

IV. ANALYSIS AND DISCUSSION

In a previous work,[12] we developed a model to calculate the change in the induced signal at the secondary coil (ΔV) with the proposed configuration as a function of the magnetic permeability of the material without any perturbation (μ_r) and the change induced by a perturbation ($\Delta\mu_r$) that could be, for instance, that is associated with internal stress. The applied model assumes monotonic behavior in the stress–strain curves, while it has been observed that low-carbon steels exhibit non-monotonic behavior in stress–strain curves.[18,19] Usually, such an effect is observed for strains above $10-2$, that is, two orders of magnitude above those induced in our experiments. Hence, we can assume linear and monotonic behavior of the curves. Nevertheless, for those low-carbon steels, a non-monotonic effect of the stress on the magnetic permeability has been observed for stresses as low as 40 MPa,[20] confirming the magneto-elastic coupling we analyze here.

In particular, we found

$$\frac{\Delta V}{V} = -\frac{1}{2}\frac{\Delta\mu_r}{\mu_r} - \psi\frac{\Delta\mu_r}{\sqrt{\mu_r}}, \tag{1}$$

where V is the voltage at the secondary coil in the absence of perturbation and $\psi = \sqrt{i\omega\sigma\mu_0 d^2}$, with ω, σ, and d, the frequency of the signal, the conductivity, and the thickness of the steel specimen, respectively.

We know that

$$\begin{aligned}\psi &= \sqrt{i\omega\sigma\mu_0 d^2} = \psi_R + i\psi_I \\ &= \frac{1}{\sqrt{2}}\sqrt{\omega\sigma\mu_0 d^2} + \frac{i}{\sqrt{2}}\sqrt{\omega\sigma\mu_0 d^2}.\end{aligned} \tag{2}$$

In the absence of perturbation, we can assume the signal induced in the secondary coil (V) to be

$$V = Ae^{i(wt+\alpha)}. \tag{3}$$

While in the presence of the perturbation, the signal induced in the secondary coil (V′) results in

$$V' = Be^{i(wt+\alpha+\Delta\alpha)}. \tag{4}$$

Hence,

$$\frac{V'}{V} = \frac{B}{A}e^{i\Delta\alpha}, \tag{5}$$

i.e., the phase of V′/V is that induced by the perturbation.

For 1 KHz, we can assume μ_r (and, consequently, $\Delta\mu_r$) to be real. Consequently,

$$\frac{V'}{V} = \frac{V+\Delta V}{V} = 1 + \frac{\Delta V}{V} = 1 - \frac{1}{2}\frac{\Delta\mu_r}{\mu_r} - \psi_R\frac{\Delta\mu_r}{\sqrt{\mu_r}} - i\psi_I\frac{\Delta\mu_r}{\sqrt{\mu_r}}. \tag{6}$$

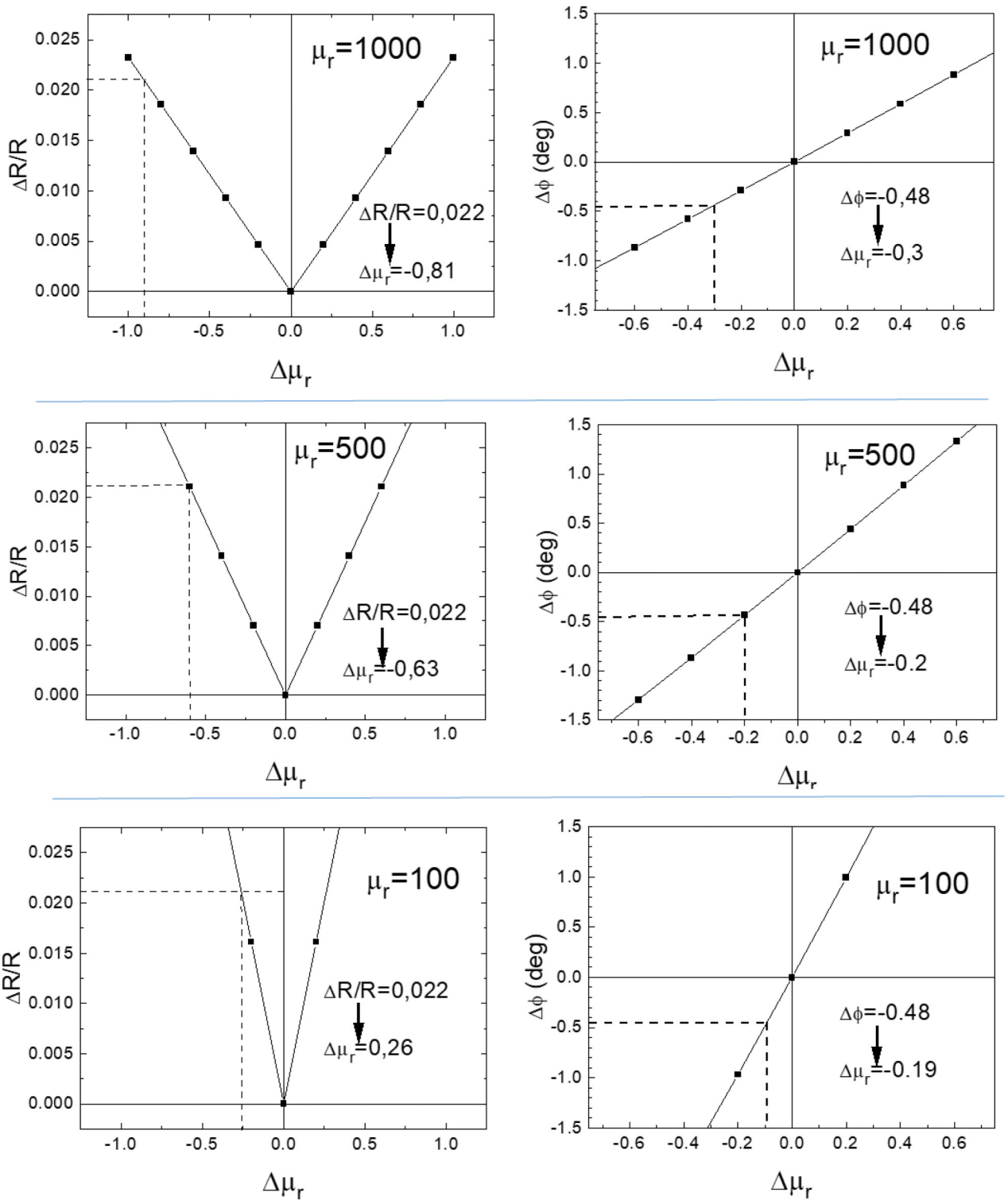

FIG. 4. Dependence of the intensity and phase of the induced signal as a function of the variation of magnetic permeability according to the proposed model. Dashed lines indicate the change of permeability that could account for the observed variations of the induced signal according to the proposed model.

The modulus and phase of V′/V are given by

$$\left|\frac{V'}{V}\right| = \sqrt{\left(1 - \frac{1}{2}\frac{\Delta\mu_r}{\mu_r} - \psi_R\frac{\Delta\mu_r}{\sqrt{\mu_r}}\right)^2 + \left(\psi_I\frac{\Delta\mu_r}{\sqrt{\mu_r}}\right)^2}, \quad (7)$$

$$\Delta\alpha = \text{arctg}\frac{\psi_I\left(\Delta\mu_r/\sqrt{\mu_r}\right)}{1 - (1/2)(\Delta\mu_r/\mu_r) - \psi_R\left(\Delta\mu_r/\sqrt{\mu_r}\right)}. \quad (8)$$

The values of μ_r reported in the literature for the steel S235 family show some dispersion depending on the processing method, but they range between 100 and 1000 depending on the processing method and mechanical treatments.[21,22] Figure 4 presents the results of the calculation of modulus and dephasing according to Eqs. (7) and (8) for μ_r values between 100 and 1000.

From those calculations and with the experimental values of modulus and dephasing, we can estimate the change of magnetic permeability induced by the applied stress (see Fig. 4). In all the cases, the values of $\Delta\mu_r$ are in the same order of magnitude and, particularly, similar for $\mu_r = 100$, which is the expected value for the magnetic field created by the primary coil. This coincidence confirms the reliability of the model to estimate (but not the obtained precise results) of the internal stress from EM measurements.

Beyond the magnetoelastic effect associated with variations in exchange interactions and magnetocrystalline anisotropy, a change in the magnetic permeability could be due to variations of the dimensions because of altering demagnetizing factors. However, Young's modulus and Poisson's ratio for the SR235JR steel are 210 GPa and 0.30, respectively.[17] The applied stress used in the experiments (up to 100 MPa) would lead to relative compression in the applied force direction of $\sim 4.76 \times 10^{-4}$ and an expansion in the direction of the magnetic field (perpendicular to the force) of $\sim 1.43 \times 10^{-4}$.

Hence, the demagnetizing factor along the applied magnetic field direction would change from 0.762 619 17 to 0.762 604 638 (Ref. 23) upon 100 MPa compression, and this would represent a relative variation in the permeability of 2×10^{-5}, three orders of magnitude below the experimental effects observed here.

Consequently, pure dimensional effects not associated with magnetoelasticity can be disregarded.

V. CONCLUSIONS

In summary, we confirmed the reliability of the EM induction method to estimate mechanical stress and prevent failure in steel elements. Moreover, comparison of experimental results with calculations confirms the validity of the previously proposed model to estimate internal stress in those elements.

SUPPLEMENTARY MATERIAL

See the supplementary material that presents measurements of electromagnetic induction as a function of applied force in load–unload cycles for fields of 10 and 100 KHz, equivalent to those shown in Figs. 2 and 3 of this paper for 1 KHz frequency.

ACKNOWLEDGMENTS

This work has been funded by the Spanish Ministry of Science and Innovation via Project No. PID2020-114192RB-C41 and by a research Ph.D. grant by the Research Vice-rectorship of Nebrija University.

CONSULTRANS SL and, in particular, its R + D + I department are acknowledged for fruitful discussions and collaboration.

AUTHOR DECLARATIONS

Conflict of Interest

The authors have no conflicts to disclose.

Author Contributions

M. A. García: Conceptualization (lead); Funding acquisition (equal); Investigation (lead); Software (lead); Writing – original draft (lead). **J. Vinolas:** Conceptualization (equal); Supervision (equal); Writing – review & editing (equal). **M. S. Garcia Alonso:** Conceptualization (equal); Investigation (equal); Methodology (equal). **A. Hernando:** Conceptualization (equal); Validation (equal); Writing – review & editing (equal).

DATA AVAILABILITY

The data that support the findings of this study are available from the corresponding author upon reasonable request.

REFERENCES

[1]J. Schlegel, *The World of Steel, on the History, Production and Use of a Basic Material* (Springer Nature, Germany, 2023).
[2]L. Holappa, "A general vision for reduction of energy consumption and CO_2 emissions from the steel industry," Metals **10**, 1117 (2020).
[3]H. Muslemani, X. Liang, K. Kaesehage, F. Ascui, and J. Wilson, "Opportunities and challenges for decarbonizing steel production by creating markets for 'green steel' products," J. Cleaner Prod. **315**, 128127 (2021).
[4]A. del Moral, *Magnetostriction: Basic Principles and Materials* (IOP Publishing, 2003).
[5]D. C. Jiles, "Review of magnetic methods for nondestructive evaluation," NDT Int. **21**, 311–319 (1988).
[6]M. K. Devine, D. C. Jiles, A. R. Eichmann, D. A. Kaminski, and S. Hardwick, "Magnescope: Applications in nondestructive evaluation," J. Appl. Phys. **21**, 5617–5619 (1993).
[7]J. M. Makar and B. K. Tanner, "The *in situ* measurement of the effect of plastic deformation on the magnetic properties of steel: Part II—permeability curves," J. Magn. Magn. Mater. **187**, 353–365 (1998).
[8]P. Vourna, A. Ktena, P. E. Tsakiridis, and E. Hristoforou, "An accurate evaluation of the residual stress of welded electrical steels with magnetic Barkhausen noise," Measurement **71**, 31 (2015).
[9]H. Kwun, "A nondestructive measurement of residual bulk stresses in welded steel specimens by use of magnetically induced velocity changes for ultrasonic waves," Mater. Eval. **44**, 1560–1566 (1986).
[10]M. S. García Alonso, F. Giacomone, A. Pérez, I. Kaiser, J. F. Fernández, A. Hernando, J. Vinolas, and M. A. García, "Magnetostatic determination of variations of internal stress in magnetic steels," AIP Adv. **10**, 115302 (2020).
[11]M. S. García Alonso, A. Hernando, J. Vinolas, and M. A. Garcia, "Magnetic detection of high mechanical stress in iron-based materials using eddy currents and phase shift measurements," J. Appl. Phys. **129**, 243901 (2021).
[12]A. Hernando, F. Giacomone, J. Viñolas, M. A. García, F. Gálvez, A. Castellanos, A. de Hoyos, and A. Cerracín, "Detecting magnetic permeability

and electrical conductivity fluctuations in metallic ferromagnetic sheets through the shielding effect," Phys. Status Solidi B **259**, 2100446 (2022).
[13]U. Aydin *et al.*, "Modeling the effect of multiaxial stress on magnetic hysteresis of electrical steel sheets: A comparison," IEEE Trans. Mag. **53**, 1 (2017).
[14]D. Buchenau, G. Schmidt, and S. Eckert, "Contact-less magneto-elastic torsional sensor based on phase-shift measurements," Meas. Sci. Technol. **25**, 075901 (2014).
[15]A. Hernando, V. Madurga, and M. Vazquez, "Magnetoelastic hysteresis of torsion," An. Fís. **72**, 253 (1976).
[16]B. D. Cullity and C. D. Graham, *Introduction to Magnetic Materials*, 2nd ed. (Wiley, 2009), Chap. 8.
[17]A. Kaľavský, P. Palička, R. Huňady, and M. Kicko, Acta Mech. Slov. **25**, 36 (2021).
[18]K. H. Nip, L. Gardner, C. M. Davies, and A. Y. Elghazouli, "Extremely low cycle fatigue tests on structural carbon steel and stainless steel," J. Constr. Steel Res. **66**, 96 (2010).
[19]A. N. Mushnikov *et al.*, "The effect of elastic deformation on the minor hysteresis loops of low carbon steel," IOP Conf. Ser.: Mater. Sci. Eng. **966**, 012055 (2020).
[20]L. G. da Silva, A. Abderahmane, M. Domenjoud, L. Bernard, and L. Daniel, "An extension of the vector-play model to the case of magneto-elastic loadings," IEEE Access **10**, 126674 (2022).
[21]M. Domenjoud and L. Daniel, "Effects of plastic strain and reloading stress on the magnetomechanical behavior of electrical steels: Experiments and modeling," Mech. Mater. **176**, 104510 (2023).
[22]E. Hristoforou, A. Ktena, P. Vourna, and K. Argiris, "Dependence of magnetic permeability on residual stresses in alloyed steels," AIP Adv. **8**, 047201 (2018).
[23]Calculated using the tool available at http://www.magpar.net/static/magpar/doc/html/demagcalc.html.